

Backflow for open quantum systems of two identical particles

S. V. Mousavi*

*Department of Physics, University of Qom,
Ghadir Blvd., Qom 371614-6611, Iran*

S. Miret-Artés†

*Instituto de Física Fundamental, Consejo Superior de
Investigaciones Científicas, Serrano 123, 28006 Madrid, Spain*

Abstract

In this work, quantum backflow for open quantum systems of two identical spinless particles is addressed within the Caldeira-Leggett (CL) approach under the presence of an opposing force and by using single Gaussian and non-Gaussian wave packets. Backflow is shown to be reduced for small opposing forces, relaxation rate, temperature and a certain degree of non-Gaussianity, but never suppressed. This effect seems to be persistent at long times when considering only one wave packet, implying that interference plays no role. This remarkable behavior is attributed to the time dependence of the width of the probability density expressed in terms of relaxation rate and temperature through the diffusion coefficient. For identical spinless particles, the so-called single-particle probability density and simultaneous/joint detection probability are evaluated. Backflow is found to be occurred only for the dissipative case, being again persistent in time only without an opposing force. Our calculations show that identical spinless fermions display a higher amount of backflow with respect to identical spinless bosons and distinguishable particles. With damping and temperature, the decoherence process, loss of being indistinguishable, is settled gradually with time. At decoherence, the nature of the particles is no longer relevant.

*Electronic address: vmousavi@qom.ac.ir

†Electronic address: s.miret@iff.csic.es

I. INTRODUCTION

One of the purely quantum effects far less known than the tunneling effect is the so-called quantum backflow. This counter-intuitive effect takes place when an ensemble of free particles described by one-dimensional wave function, located in the negative axis of the coordinate and possessing only positive momenta, displays a non-decreasing probability of remaining in the negative region during certain periods of time. This effect was due to Allcock [1] when studying arrival times in quantum mechanics. Bracken and Melloy [2] carried out subsequently a systematic and detailed study of this effect by providing an upper limit to the probability which can flow back from positive to negative values of the coordinate to be around 0.04. No backflow has been reported for a single Gaussian wave packet implying that this effect is related to an interference process [3]. No experimental evidence of this effect has been reported yet, though a feasible experimental scheme based on imprinting the backflow on a Bose-Einstein condensate and detecting the effect by a usual density measurement has been proposed [4]. This maximum amount of probability occurring in general over any finite time interval seems to be independent on the time interval, particle mass and Planck constant, talking about a new dimensionless quantum number was found. The same authors [5] have also studied this effect in the presence of a constant field and in relativistic quantum mechanics from the Dirac equation. Interestingly enough, they also formulated the probability flow in terms of an eigenvalue problem of the flux operator. In continuation of these studies, optimization numerical problems were reported by Penz et al. [6]. Superoscillations [7] and weak values [8] have also been related to this effect by Berry. In a different context, Yearsley et al. [9, 10] analyzed and discussed the classical limit as well as some specific measurement models. Following the work by Bracken and Melloy, Albarelli *et al.* considered the notion of nonclassicality arising from the backflow effect and analyzed its relationship with the negativity of the Wigner function [11]. Backflow has also been studied, under the presence of a constant field, and shown that it is mathematically equivalent to the problem of diffraction in time [12] for particles initially confined to a semi-infinite line and expanding them later on in free space [13]. Backflow has also been extended to scattering problems in short-range potentials where it has been shown that this effect is a universal quantum one [14].

Curiously, very few studies have been carried out in the context of open quantum systems.

Yearsley has analyzed the arrival time problem in the framework of decoherent histories for a particle coupled to an environment [15]. Recently, we have carried out the dynamics of backflow in terms of damping and temperature and addressed this issue within two different frameworks [16], the Caldirola-Kanai [17] and the Caldeira-Leggett (CL) [18, 19] approaches. Backflow has been shown to be reduced with dissipation and temperature but never suppressed. Moreover, quantum backflow has been surprisingly observed for a single Gaussian wave packet within the CL formulation and a constant force acting against backflow. Interestingly enough, this effect seems to be persistent at long times when considering both one and two Gaussian wave packets within the CL context. For the case of a single Gaussian wave packet, this is a clear indication that backflow is no longer due to an interference process. This remarkable behavior has been attributed to the time behavior of the width of the probability density in terms of damping and temperature through the diffusion coefficient. The classical limit of backflow within the context of the classical Schrödinger equation [20] has also been shown to be present.

Following this previous work, we have tackled the same theoretical analysis by extending the study to more general stretching Gaussian and non-Gaussian wave packets and to systems of two identical spinless particles. For identical spinless particles, the so-called single-particle probability density and simultaneous/joint detection probability are evaluated for the different quantum statistics. Backflow is found to be occurred only in the dissipative case and reduced for small opposing forces, relaxation time, temperature and a certain degree of non-Gaussianity, but never suppressed in the free propagation limit. Interestingly enough, identical spinless fermions, being described by an anti-symmetric wave function, display a higher amount of backflow than identical spinless bosons, being described by a symmetric wave function, and distinguishable particles. It seems that the well-known properties of bunching for bosons and anti-bunching for fermions tend to disappear when compared to distinguishable particles. In other words, with damping and temperature, the decoherence process, loss of being indistinguishable, is settled gradually with time. At decoherence, the nature of the particles is no longer relevant.

This work is organized as follows. In Section I, the time evolution of the reduced density matrix governed by the CL master equation is briefly introduced. Section II is devoted to analyze the quantum backflow through the time behavior of different wave packets under the presence of a general linear potential, the non-minimum-uncertainty-product Gaussian wave

packet and two non-Gaussian wave packets simulating the first two excited states of a simple harmonic oscillator. Section III is devoted to deal with the backflow for identical particles following different quantum statistics. In Section V, some numerical results are presented and discussed. Finally, in the last section, a summary and some conclusions derived from this work are given.

II. THE CALDEIRA-LEGGETT MASTER EQUATION

Open quantum systems can be dealt within the so-called *system-plus-environment approach* where the total system is considered to be isolated. The total system is described by a pure state, a wave function, whose evolution is determined by the unitary time evolution operator fulfilling the usual Schrödinger equation. Within the density matrix formalism, the total density matrix is expressed by the direct product of the density matrices of both, the system of interest (or simply, the system) and environment. The reduced density matrix ρ describing the system of interest is obtained by tracing out the degrees of freedom of the environment. In this way, a master equation is derived for the evolution of the reduced density which contains both frictional and thermal effects due to the presence of the environment. The Caldeira-Leggett [18] formalism is an example of the above approach where the environment is modelled by a bosonic bath, consisting of an infinite number of quantum oscillators in thermal equilibrium, and interacts with the system through a coupling expressed in terms of distances. In this framework, the Brownian motion is reproduced in the classical regime and, in this sense, this bath is actually a minimal one [19]. This formalism has recently been used to describe interference and diffraction of identical particles [21] and dissipative quantum backflow [16]. The corresponding Markovian master equation in the coordinate representation, at the high temperature limit $\hbar\gamma \ll k_B T$, where γ is the relaxation rate and k_B is the Boltzman constant, takes the simple form in one-dimension [18, 19, 22]

$$\frac{\partial \rho(x, x', t)}{\partial t} = \left[-\frac{\hbar}{2mi} \left(\frac{\partial^2}{\partial x^2} - \frac{\partial^2}{\partial x'^2} \right) - \gamma(x - x') \left(\frac{\partial}{\partial x} - \frac{\partial}{\partial x'} \right) + \frac{V(x) - V(x')}{i\hbar} - \frac{D}{\hbar^2} (x - x')^2 \right] \rho(x, x', t) \quad (1)$$

where

$$D = 2m\gamma k_B T \quad (2)$$

plays the role of a diffusion coefficient and $V(x)$ represents the interaction potential. In the center of mass and relative coordinates

$$\begin{cases} R = \frac{x + x'}{2} \\ r = x - x'. \end{cases} \quad (3a)$$

$$(3b)$$

Eq. (1) can be rewritten as

$$\frac{\partial \rho}{\partial t} + \frac{\partial j}{\partial R} + \frac{V(R/2 + r) - V(R/2 - r)}{i\hbar} + 2\gamma r \frac{\partial \rho}{\partial r} + r^2 \frac{D}{\hbar^2} \rho = 0 \quad (4)$$

where the current density matrix is defined by

$$j(R, r, t) = -i \frac{\hbar}{m} \frac{\partial}{\partial r} \rho(R, r, t). \quad (5)$$

Diagonal elements of the density matrix has the interpretation of the probability density.

By imposing the condition $r = 0$ in Eq. 4, the continuity equation emerges according to

$$\frac{\partial P(x, t)}{\partial t} + \frac{\partial J(x, t)}{\partial x} = 0, \quad (6)$$

where $P(x, t)$ and $J(x, t)$ give the diagonal elements of $\rho(R, r, t)$ and $j(R, r, t)$, respectively.

The probability that the particle can be found in the region $(-\infty, 0]$ is

$$\Pr(x \leq 0, t) = \int_{-\infty}^0 P(x, t) dx \quad (7)$$

and according to the continuity equation

$$\frac{\Pr(x \leq 0, t)}{dt} = -J(0, t) \quad (8)$$

provided that $J(-\infty, 0) = 0$. In general, $J(0, t) \geq 0$ for $t \geq 0$ and therefore $\Pr(x \leq 0, t)$ is a decreasing function with time in the time interval $(-\infty, 0]$. However, if there are some time intervals where $J(0, t)$ is negative, the corresponding probability is increasing and we have the hallmark of backflow.

III. LINEAR POTENTIAL AND GAUSSIAN AND NON-GAUSSIAN WAVE PACKETS

In this section we are going to solve the CL master equation with a linear potential for initial wave packets having the shape of non-minimum-uncertainty-product Gaussian and also two specific forms of non-Gaussian wave packets.

A. Non-minimum-uncertainty-product Gaussian wave packet

Let us first consider the initial state to be a non-minimum-uncertainty-product Gaussian wave packet (or simply stretched Gaussian wave packet) given by

$$\psi_0(x) = \frac{1}{(2\pi\sigma_0^2(1+i\eta)^2)^{1/4}} \exp \left[-\frac{(x-x_0)^2}{4\sigma_0^2(1+i\eta)} + i\frac{p_0}{\hbar}x \right], \quad (9)$$

where η is the stretching parameter and σ_0 , x_0 and p_0 are the initial width, position and momentum, respectively. The master equation (1) under the presence of the linear potential $V(x) = m g x$ can be analytically solved. The Gaussian wave packet given by Eq. (9) is the non-minimum-uncertainty-product Gaussian wave packet in the sense that the product $\Delta x \Delta p$ does not have the minimum value $\hbar/2$, where $\Delta x = \sigma_0 \sqrt{1+\eta^2}$ and $\Delta p = \hbar/2\sigma_0$ are the uncertainties in position and momentum, respectively. The solution of this equation in the center of mass and relative coordinates (3a) and (3b) is reached by using the technique of the Fourier transform with respect to the center of mass coordinate, solving the resulting equation and then taking the inverse Fourier transform of this solution in order to obtain the density matrix in the position representation [22, 23]. In this way, we have

$$\rho(R, r, t) = \frac{1}{\sqrt{2\pi}w_t} \exp \left[a_0(r, t) - \frac{(R - a_1(r, t))^2}{2w_t^2} \right], \quad (10)$$

$$j(R, r, t) = -i\frac{\hbar}{m} \left(\frac{\partial a_0}{\partial r} + \frac{x - a_1(0, t)}{w_t^2} \frac{\partial a_1}{\partial r} \right) \rho(R, r, t) \quad (11)$$

for the density matrix and current density matrix, respectively, where the following definitions are used

$$a_0(r, t) = - \left[\frac{e^{-4\gamma t}}{8\sigma_0^2} + \frac{1 - e^{-4\gamma t}}{4\gamma} \frac{D}{\hbar^2} \right] r^2 + i \left(\frac{p_0}{\hbar} e^{-2\gamma t} - \frac{mg}{\hbar} \frac{1 - e^{-2\gamma t}}{2\gamma} \right) r, \quad (12)$$

$$a_1(r, t) = x_t + i \left[\frac{\hbar}{4m\sigma_0^2} e^{-2\gamma t} \frac{1 - e^{-2\gamma t}}{2\gamma} + \frac{D}{m\hbar} \left(\frac{1 - e^{-2\gamma t}}{2\gamma} \right)^2 + \frac{\eta}{2} e^{-2\gamma t} \right] r, \quad (13)$$

$$w_t = \sigma_0 \sqrt{1 + \frac{\hbar^2}{4m^2\sigma_0^4} \left(\frac{1 - e^{-2\gamma t}}{2\gamma} \right)^2 + \frac{4\gamma t + 4e^{-2\gamma t} - 3 - e^{-4\gamma t}}{8m^2\gamma^3\sigma_0^2} D + \eta \frac{\hbar}{m\sigma_0^2} \frac{1 - e^{-2\gamma t}}{2\gamma} + \eta^2}, \quad (14)$$

and where γ and D (and therefore, the temperature) appear in the three time functions. However, the linear potential ruled by the g parameter appears explicitly in the $a_0(r, t)$ function and also in $a_1(r, t)$ via x_t where

$$x_t = x_0 + \frac{p_0}{m} \frac{1 - e^{-2\gamma t}}{2\gamma} - g \frac{2\gamma t - 1 + e^{-2\gamma t}}{4\gamma^2}, \quad (15)$$

the η parameter being involved in the $a_1(r, t)$ and w_t functions. Now, by substituting Eqs. (12), (13) and (14) into Eqs. (10) and (11) and imposing the condition $r = 0$, one yields

$$P(x, t) = \frac{1}{\sqrt{2\pi}w_t} \exp \left[-\frac{(x - x_t)^2}{2w_t^2} \right], \quad (16)$$

$$J(x, t) = \left\{ \frac{p_0}{m} e^{-2\gamma t} - g \frac{1 - e^{-2\gamma t}}{2\gamma} + \frac{x - x_t}{w_t^2} \right. \\ \left. \left[\frac{1 - e^{-2\gamma t}}{2\gamma} \left(\frac{\hbar^2}{4m^2\sigma_0^2} e^{-2\gamma t} + \frac{D}{m^2} \frac{1 - e^{-2\gamma t}}{2\gamma} \right) + \eta \frac{\hbar}{2m} e^{-2\gamma t} \right] \right\} P(x, t), \quad (17)$$

for the probability density (PD) and probability current density (PCD), respectively. Equation (16) shows that the PD has a Gaussian shape with a width w_t given by Eq. (14) and a center moving along the *classical* trajectory x_t given by Eq. (15).

In the zero dissipation limit, the second term on the right hand side of Eq.(1), i.e., the term proportional to the damping constant, can be neglected. In this limit, Eqs. (15) and (14) reduce to

$$x_t \approx x_0 + \frac{p_0}{m}t - \frac{1}{2}gt^2, \quad (18)$$

$$w_t \approx \sigma_0 \sqrt{1 + \frac{\hbar^2}{4m^2\sigma_0^4}t^2 + \frac{2D}{3m^2\sigma_0^2}t^3 + \eta \frac{\hbar}{m\sigma_0^2}t + \eta^2}. \quad (19)$$

Note that this limit corresponds to short times where $\gamma t \ll 1$, i.e., times much shorter than the relaxation time [15].

B. Non-Gaussian wave packets

Now suppose the wave function has the non-Gaussian form

$$\psi_0(x) = \frac{x - x_0}{\sigma_0} \frac{1}{(2\pi\sigma_0^2)^{1/4}} \exp \left[-\frac{(x - x_0)^2}{4\sigma_0^2} + i\frac{p_0}{\hbar}x \right]. \quad (20)$$

This state can be considered as the first excited state of a simple harmonic oscillator by imposing $p_0 = 0$ and $\sigma_0 = \sqrt{2m\omega/\hbar}$. The solution of the master equation (1) via the method outlined above yields

$$\rho(R, r, t) = \frac{w_t^4 d_0(r, t) - d_2(t)(R - b_1(r, t))^2 + w_t^2 [d_2(t) - id_1(r, t)(R - b_1(r, t))]}{w_t^5} \\ \times \exp \left[b_0(r, t) - \frac{(R - b_1(r, t))^2}{2w_t^2} \right] \quad (21)$$

for the elements of the density matrix in the position representation where

$$b_0(r, t) = a_0(r, t) - 4\gamma t, \quad (22)$$

$$b_1(r, t) = a_1(r, t)|_{\eta=0}, \quad (23)$$

$$d_0(r, t) = \frac{1}{\sqrt{2\pi}} \left(e^{4\gamma t} - \frac{r^2}{4\sigma_0^2} \right), \quad (24)$$

$$d_1(r, t) = \frac{1}{\sqrt{2\pi}} \frac{\hbar}{2m\sigma_0^2} \frac{1 - e^{2\gamma t}}{2\gamma} r, \quad (25)$$

$$d_2(t) = -\frac{1}{\sqrt{2\pi}} e^{4\gamma t} \sigma_0^2 \left(1 - \frac{\hbar^2}{16m^2\gamma^2\sigma_0^4} (1 - 2e^{-2\gamma t} + e^{-4\gamma t}) \right), \quad (26)$$

and w_t given by Eq. (14).

If we now consider another form of non-Gaussian wave packet such as

$$\psi_0(x) = \frac{(x - x_0)^2}{\sqrt{3}\sigma_0^2} \frac{1}{(2\pi\sigma_0^2)^{1/4}} \exp \left[-\frac{(x - x_0)^2}{4\sigma_0^2} + i\frac{p_0}{\hbar}x \right], \quad (27)$$

which with $p_0 = 0$ would correspond to the second excited state of a simple harmonic oscillator with $\omega = \sqrt{\hbar/2m\sigma_0^2}$, then the solution of the CL master equation yields

$$\rho(x, t) = \frac{A_0(t) + A_1(t)x + A_2(t)x^2 + A_3(t)x^3 + A_4(t)x^4}{4w_t^9} \exp \left[-8\gamma t - \frac{(x - x_t)^2}{2w_t^2} \right] \quad (28)$$

for PD, diagonal elements of the density matrix, with

$$A_0(t) = \frac{e^{8\gamma t}}{\sqrt{2\pi}} + f_2(t)w_t^4(w_t^2 - x_t^2) + f_4(t)\{3w_t^4 - 6w_t^2x_t^2 + x_t^4\}, \quad (29)$$

$$A_1(t) = 2x_t\{f_2(t)w_t^4 + 2f_4(t)(3w_t^2 - x_t^2)\}, \quad (30)$$

$$A_2(t) = -f_2(t)w_t^4 - 6f_4(t)(w_t^2 - x_t^2), \quad (31)$$

$$A_3(t) = -4f_4(t)x_t, \quad (32)$$

$$A_4(t) = f_4(t), \quad (33)$$

and

$$f_2(t) = -\sqrt{\frac{2}{\pi}} e^{8\gamma t} \sigma_0^2 \left\{ 1 + \frac{\hbar^2}{12m^2\sigma_0^2} \left(\frac{1 - e^{-2\gamma t}}{2\gamma} \right)^2 \right\}, \quad (34)$$

$$f_4(t) = -\frac{1}{\sqrt{2\pi}} e^{8\gamma t} \sigma_0^4 \left\{ 1 + \frac{\hbar^2}{4m^2\sigma_0^2} \left(\frac{1 - e^{-2\gamma t}}{2\gamma} \right)^2 \right\}. \quad (35)$$

IV. QUANTUM BACKFLOW

The quantum backflow effect is a counter-intuitive fact, a pure quantum effect where a state consisting of negligible negative momentum exhibits negative probability flux over some time intervals at a given point, e.g., the origin. Thus, the probability of finding the quantum system to the left of the origin increases during these time intervals. In this section we first address this problem for single-particle systems and then extend the study to systems of two-identical particles, bosons and fermions in order to see how the quantum statistics influence such an effect.

A. One particle systems

In the context of isolated quantum systems described by the Schrödinger equation, it has been shown that the backflow effect can not take place for a single Gaussian wave packet [9] but by two wave packets, meaning that this phenomenon is due to an interference process [13]. However, we have recently shown the occurrence of this effect in the free propagation of a *single Gaussian* wave packet within the CL framework. We want to extend this study when a linear potential is considered for more general stretching Gaussian and non-Gaussian wave packets.

Let us assume a system described initially by the stretching Gaussian wave packet (9) with $x_0 = 0$. Then, the probability of finding a negative value in a measurement of momentum is given by [16]

$$\Pr(p \leq 0, 0) = \frac{1}{2} \operatorname{erfc} \left[\sqrt{2} \frac{p_0 \sigma_0}{\hbar} \right]. \quad (36)$$

which is a function of the initial parameters p_0 and σ_0 . One should choose parameters of the wave packet in such a way that this probability becomes negligible. From the time evolution of the PD (16), one obtains

$$\Pr(x \leq 0, t) = \frac{1}{2} \operatorname{erfc} \left[\frac{x_t}{\sqrt{2} w_t} \right] \quad (37)$$

for the probability of finding the particle to the left of the origin, $x \leq 0$. The quantum backflow occurs in time intervals where the argument of the complementary error function is decreasing (the argument $\frac{x_t}{\sqrt{2} w_t}$ is not essentially an increasing function of time). From

Eqs. (14) and (15), one has that

$$w_t \Big|_{\gamma t \gg 1} \approx \sqrt{\frac{k_B T}{m\gamma}} t \quad (38)$$

$$x_t \Big|_{\gamma t \gg 1} \approx -\frac{g}{2\gamma} t \quad (39)$$

at long times. From these relations, one sees that the probability $\Pr(x \leq 0, t)$ in the absence of the linear potential, $g = 0$, approaches 0.5 when $\gamma t \gg 1$, while it vanishes with the presence of a constant force. This means that the time interval of the backflow is semi-infinite for $g = 0$ while it is finite, if there is any, for non-zero g values.

In the zero dissipation limit and for $g = 0$ and $\eta = 0$, the argument of the complementary error function in Eq. (37) reaches a maximum at time

$$t_m = \left(\frac{3m\sigma_0^2}{2\gamma k_B T} \right)^{1/3} \quad (40)$$

which is shorter for higher temperatures. At this time, $\Pr(x \leq 0, t)$ becomes a minimum. This means there is only a time interval for backflow, $[t_m, \infty)$, which is longer for higher temperatures. Even more, the backflow is persistent at asymptotic times. The argument of the complementary error function at $t = t_m$ is a decreasing function of temperature, thus $\Pr(x \leq 0, t_m)$ increases with temperature and therefore the *amount of backflow* quantified by the difference $\Pr(x \leq 0, \infty) - \Pr(x \leq 0, t_m)$ decreases with temperature.

When the system is described by the non-Gaussian wave packet (20), one obtains

$$\Pr(p \leq 0, 0) = \frac{1}{2} \operatorname{erfc} \left[\sqrt{2} \frac{p_0 \sigma_0}{\hbar} \right] + \sqrt{\frac{2}{\pi}} \frac{p_0 \sigma_0}{\hbar} \exp \left[-2 \frac{p_0^2 \sigma_0^2}{\hbar^2} \right], \quad (41)$$

$$\Pr(x \leq 0, t) = \frac{1}{2} \operatorname{erfc} \left[\frac{x_t}{\sqrt{2} w_t} \right] - d_2(t) \frac{x_t}{w_t^3} \exp \left[-2\gamma t - \frac{x_t^2}{2w_t^2} \right] \quad (42)$$

where x_t , w_t and $d_2(t)$ are given by Eqs. 15), (14) and (26), respectively. As mentioned above, one should choose parameters of the wave packet in such a way that $\Pr(p \leq 0, 0)$ becomes negligibly small, i.e., the wave packet is *practically* constructed from positive momenta. On the other hand, for the the non-Gaussian wave packet (27), the probability of backflow is given by

$$\Pr(p \leq 0, 0) = \frac{1}{2} \operatorname{erfc} \left[\sqrt{2} \frac{p_0 \sigma_0}{\hbar} \right] - \sqrt{\frac{2}{\pi}} \frac{p_0 \sigma_0}{\hbar} \left(1 - 4 \frac{p_0^2 \sigma_0^2}{\hbar^2} \right) \exp \left[-2 \frac{p_0^2 \sigma_0^2}{\hbar^2} \right], \quad (43)$$

$$\Pr(x \leq 0, t) = \frac{1}{2} \operatorname{erfc} \left[\frac{x_t}{\sqrt{2} w_t} \right] - \frac{x_t \{ f_2(t) w_t^4 + f_4(t) (3w_t^2 - x_t^2) \}}{w_t^7} \exp \left[-8\gamma t - \frac{x_t^2}{2w_t^2} \right] \quad (44)$$

where x_t , w_t , $f_2(t)$ and $f_4(t)$ are given by Eqs. (15), (14), (34) and (35), respectively.

B. Two identical particles

In a system of two identical particles, the state describing the system must have a given symmetry; anti-symmetric for fermions (following the Fermi-Dirac (FD) statistics) and symmetric for bosons (following the Bose-Einstein (BE) statistics) under the exchange of particles. Let us consider a system of two identical spinless particles described initially by the pure state

$$\Psi_{\pm}(x_1, x_2, 0) = N_{\pm}[\psi_a(x_1, 0)\psi_b(x_2, 0) \pm \psi_a(x_2, 0)\psi_b(x_1, 0)] \quad (45)$$

where the sub-indices $+$ and $-$ refer to bosons and fermions, respectively. By taking the initial single-particle states as co-centered Gaussian wave packets, Eq. (9) with $\eta = 0$, centered at the origin, and having the kick momenta p_{0a} and p_{0b} , the normalization constant N_{\pm} is then given by

$$N_{\pm} = \left(2 \pm 2 e^{-(p_{0a}-p_{0b})^2 \sigma_0^2 / \hbar^2}\right)^{-1/2}. \quad (46)$$

With this initial state, the probability of obtaining negative values for the momenta of both particles in a simultaneous measurement of momenta is given by

$$\begin{aligned} \text{Pr}_{\pm}(0) \Big|_{p_1 \& p_2 \in (-\infty, 0]} &= \int_{-\infty}^0 dp'_1 \int_{-\infty}^0 dp'_2 |\Phi_{\pm}(p'_1, p'_2, 0)|^2 = \frac{N_{\pm}^2}{2} e^{-(p_{0a}-p_{0b})^2 \sigma_0^2 / 2\hbar^2} \\ &\times \left(e^{\mp(p_{0a}-p_{0b})^2 \sigma_0^2 / 2\hbar^2} \text{erfc} \left[\frac{(p_{0a} + p_{0b})\sigma_0}{\sqrt{2}\hbar} \right] \right. \\ &\left. \pm e^{\pm(p_{0a}-p_{0b})^2 \sigma_0^2 / 2\hbar^2} \text{erfc} \left[\sqrt{2} \frac{p_{0a}\sigma_0}{\hbar} \right] \text{erfc} \left[\sqrt{2} \frac{p_{0b}\sigma_0}{\hbar} \right] \right) \end{aligned} \quad (47)$$

where $\Phi_{\pm}(p_1, p_2, 0)$ is the Fourier transform of the initial wave function (45). The solution of the CL master equation given by Eq. (1) is then given by [21]

$$\begin{aligned} \rho_{\pm}(x_1, x'_1; x_2, x'_2, t) &= N_{\pm}^2 \{ \rho_{aa}(x_1, x'_1, t) \rho_{bb}(x_2, x'_2, t) \pm \rho_{ab}(x_1, x'_1, t) \rho_{ba}(x_2, x'_2, t) \\ &\pm \rho_{ba}(x_1, x'_1, t) \rho_{ab}(x_2, x'_2, t) + \rho_{bb}(x_1, x'_1, t) \rho_{aa}(x_2, x'_2, t) \} \end{aligned} \quad (48)$$

where $\rho_{ij}(x, x', t)$, i and j referring to a and b , is the time-evolution of $\psi_i(x, 0)\psi_j^*(x, 0)$ which can be obtained by the method outlined above. Just for comparison, for distinguishable particles obeying the Maxwell-Boltzmann (MB) statistics, the density matrix is given by

$$\rho_{\text{MB}}(x_1, x'_1; x_2, x'_2, t) = \frac{1}{2} \{ \rho_{aa}(x_1, x'_1, t) \rho_{bb}(x_2, x'_2, t) + \rho_{bb}(x_1, x'_1, t) \rho_{aa}(x_2, x'_2, t) \}. \quad (49)$$

Thus, the simultaneous detection probability of both particles being in the negative semi-infinite space is defined as

$$\Pr_{\pm}(t) \Big|_{x_1 \& x_2 \in (-\infty, 0]} = \int_{-\infty}^0 dy_1 \int_{-\infty}^0 dy_2 \rho_{\pm}(y_1, y_1; y_2, y_2, t) \quad (50)$$

where $\rho_{\pm}(y_1, y_1; y_2, y_2, t)$ are the diagonal elements of the two-particle density matrix (48). To evaluate this probability one must first compute the corresponding probability for each term appearing in Eq. (48) which yields

$$\Pr_{ij}(t) = \int_{-\infty}^0 dy \rho_{ij}(y, y, t) = \frac{1}{2} e^{-(p_{0i}-p_{0j})^2 \sigma_0^2 / 2\hbar^2} \operatorname{erfc} \left[\frac{\frac{x_{ti}+x_{tj}}{2} + i \frac{(p_{0i}-p_{0j})\sigma_0^2}{\hbar}}{\sqrt{2}w_t} \right] \quad (51)$$

where w_t is given by Eq. (14) and x_{ti} by Eq. (15), imposing $x_0 = 0$ and $p_0 = p_{0i}$. Then, from Eqs. (48) and (50), one has

$$\Pr_{\pm}(t) \Big|_{x_1 \& x_2 \in (-\infty, 0]} = 2N_{\pm}^2 \{ \Pr_{aa}(t) \Pr_{bb}(t) \pm \Pr_{ab}(t) \Pr_{ba}(t) \}. \quad (52)$$

On the other hand, an also interesting probability is the so-called single-particle (sp) detection probability, that is, the probability for finding a particle at $x \leq 0$ irrespective from the position of the other particle which is given by

$$\begin{aligned} \Pr_{\text{sp}, \pm}(x \leq 0, t) &= \int_{-\infty}^0 dy_1 \int_{-\infty}^{\infty} dy_2 \rho_{\pm}(y_1, y_1; y_2, y_2, t) \\ &= N_{\pm}^2 \{ \Pr_{aa}(t) \pm e^{-(p_{0a}-p_{0b})^2 \sigma_0^2 / 2\hbar^2} [\Pr_{ab}(t) + \Pr_{ba}(t)] + \Pr_{bb}(t) \} \end{aligned} \quad (53)$$

where in the second equality Eq. (48) has been used.

V. RESULTS AND DISCUSSION

Numerical calculations are carried out in atomic units, $\hbar = 1$ and $m = 1$, along this work. In Figure 1, density plots of the PCD (17) for the damping constant $\gamma = 0.1$ are shown for $k_B T = 1$ (left panel) and $k_B T = 5$ (right panel) for the free propagation of stretching Gaussian wave packet (9). From the color gradients displayed in this figure, one sees that after a certain time which depends on both temperature and the stretching parameter η , the PCD becomes negative with time. This is the hallmark of the quantum backflow.

The next step is to analyze the dynamics of the backflow under the presence of a linear potential $V(x) = mgx$ with g negative in order to have opposing forces which are against

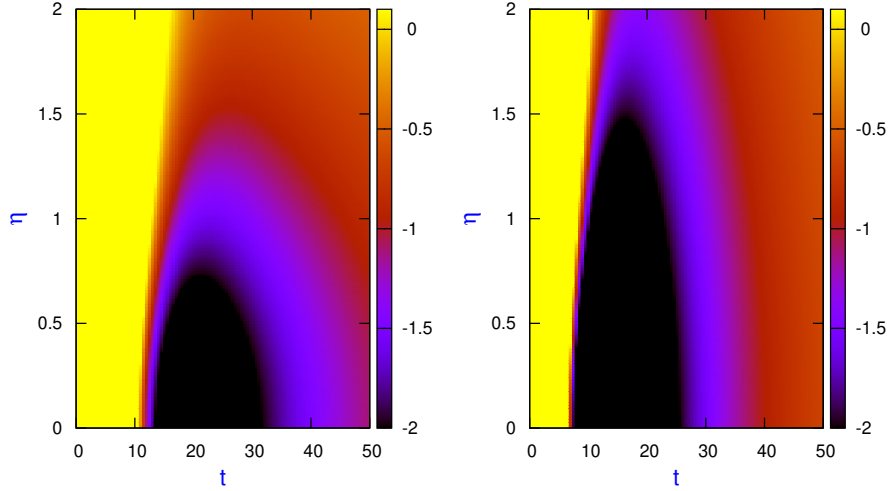


FIG. 1: Density plots of the probability current density (17) magnified by a factor of 1000 for the damping constant $\gamma = 0.1$ with $k_B T = 1$ (left panel) and $k_B T = 5$ (right panel). Parameters are chosen to be $\sigma_0 = 10$, $x_0 = 0$, $p_0 = 1.4$ and $g = 0$.

backflow. In Fig. 2 it is plotted the PD for remaining in $x \leq 0$ versus time, $\Pr(x \leq 0, t)$, for the propagation of a single Gaussian wave packet (left top panel), and two single non-Gaussian wave packets given by Eq. (20) (left middle panel) and Eq. (27) (left bottom panel) for $k_B T = 2$ with $g = 0$ (black curves), $g = -0.01$ (red curves) and $g = -0.02$ (green curves). Right panels display the same probability for $g = 0$ but with $k_B T = 3$ (right top panel), $k_B T = 5$ (right middle panel) and $k_B T = 10$ (right bottom panel) for the Gaussian wave packet (cyan curves) and the two non-Gaussian wave packets, Eqs. (20) (magenta curves) and (27) (blue curves). The initial parameters used are $\sigma_0 = 10$, $x_0 = 0$, $p_0 = 1.4$, $\eta = 0$ and $\gamma = 0.05$. For these parameter the probability of obtaining negative values for the momentum is practically zero. These calculations show that this probability is a decreasing function with time till reaching a minimum more or less pronounced (see left panels). After this minimum, the probability increases slowly reaching a certain *plateau* only for the freely propagating case. For all nonzero negative values of g , one can easily show that this probability becomes zero at long times. This means that quantum backflow is already present with a single wave packet and with small opposing forces. For higher values of g we do not observe any minimum point. In contrast to the backflow observed for superposition

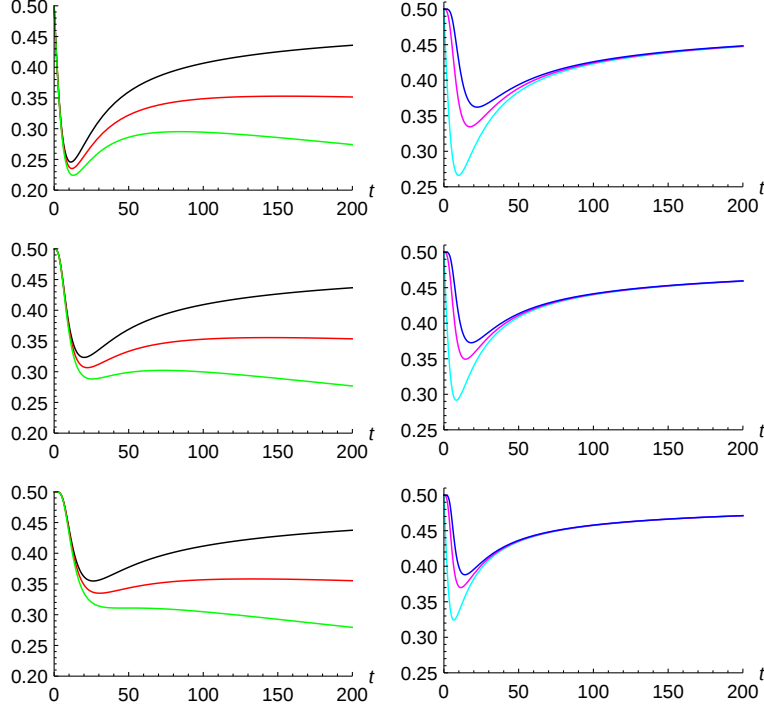


FIG. 2: The probability for remaining in $x \leq 0$ versus time, $\Pr(x \leq 0, t)$, for the propagation of a single Gaussian wave packet (left top panel), and the two single non-Gaussian wave packets given by Eq. (20) (left middle panel) and Eq. (27) (left bottom panel) under the presence of the force $-mg$ for $k_B T = 2$ with $g = 0$ (black curves), $g = -0.01$ (red curves) and $g = -0.02$ (green curves). Right panels display the same probability for $g = 0$ with $k_B T = 3$ (right top panel), $k_B T = 5$ (right middle panel) and $k_B T = 10$ (right bottom panel) for the Gaussian wave packet (cyan curves) and the two non-Gaussian wave packets, Eq. (20) (magenta curves) and Eq. (27) (blue curves). The initial parameters used are $\sigma_0 = 10$, $x_0 = 0$, $p_0 = 1.4$, $\eta = 0$ and $\gamma = 0.05$.

of two Gaussian wave packets [16] where there are several intervals of backflow, here for the single wave packets used, there is only one interval. The series expansion of location of this minimum for $g = 0$, in the negligible dissipation limit, is given by

$$t_m = \left(\frac{3m^2\sigma_0^2}{D} \right)^{1/3} + \frac{\hbar}{2} \left(\frac{m}{3\sigma_0^2 D^2} \right)^{1/3} \eta + \left(\frac{m^2\sigma_0^2}{9D} \right)^{1/3} \eta^2 + O(\eta^3). \quad (54)$$

According to the definition of D , t_m decreases with temperature for a given value of η and the backflow starts sooner for higher values of temperature. On the other hand, for a given value of temperature, t_m increases with η meaning that backflow starts later for higher values of η . Although our analysis is carried out in the negligible dissipation limit, the

numerical calculations presented in Fig. 1 show that this point is valid in general. In the same figure, $\Pr(x \leq 0, t)$ has also been plotted for both Gaussian and non-Gaussian wave packets. Backflow interval is shorter for the non-Gaussian wave packets than the Gaussian one. Actually, the backflow interval decreases with the degree of non-Gaussianity. The amplitude of this increasing in the probability has been used to quantify the amount of backflow, $\Pr(x \leq 0, t_2) - \Pr(x \leq 0, t_1)$; $[t_1, t_2]$ being the time interval where the backflow takes place. Note that $t_2 \rightarrow \infty$ for $g = 0$. From Fig. 2, it is found that the amount of backflow decreases both with temperature and acceleration g . From the right panels, we clearly see that by increasing the temperature, this probability tends to a constant at long times for all the wave packets analyzed here becoming backflow a persistent effect.

Concerning two identical spinless particles, we start discussing the existence of backflow for non-dissipative fermion and boson systems. Fig. 3 shows, in the context of the Schrödinger equation, both the single-particle (left panels) and simultaneous detection probabilities (right panels) for different statistics and g values. These probabilities are shown for $g = 0$ (top panels) and $g = -0.01$ (bottom panels) for the MB (cyan curves), BE (magenta curves) and FD (blue curves) statistics. The initial parameters used are $\sigma_0 = 10$, $x_0 = 0$, $p_{0a} = 0.3$ and $p_{0b} = 0.4$. For these parameters, the probability for finding negative values of momenta for bosons is $\sim 10^{-25}$ while for fermions is one order of magnitude smaller. In any case, these values guarantee that the corresponding initial wave functions are practically composed of positive momenta. As can be clearly observed, there is no backflow nor in the single-particle detection probability nor in the joint detection probability. The existence of an opposing force implies a faster decay of such probabilities. The single-particle detection probability of fermions is higher than that for bosons and distinguishable particles while just the opposite behavior is seen for the joint detection probability.

In the dissipative case, things are fortunately quite different. Fig. 4 shows the simultaneous detection probability, Eq. (52), for detecting both particles in the region $x \leq 0$ for different statistics for a given γ but different temperatures and negative values of g . The left panels show this probability for $k_B T = 10$ and different statistics: MB (left top panel), BE (left middle panel) and FD (left bottom panel) for $g = 0$ (black curves), $g = -0.01$ (red curves) and $g = -0.02$ (green curves). The same quantity is plotted for $g = 0$ in the right panels for different values of temperatures: $k_B T = 5$ (right top panel), $k_B T = 15$ (right middle panel) and $k_B T = 40$ (right bottom panel) for the same MB (cyan curves), BE

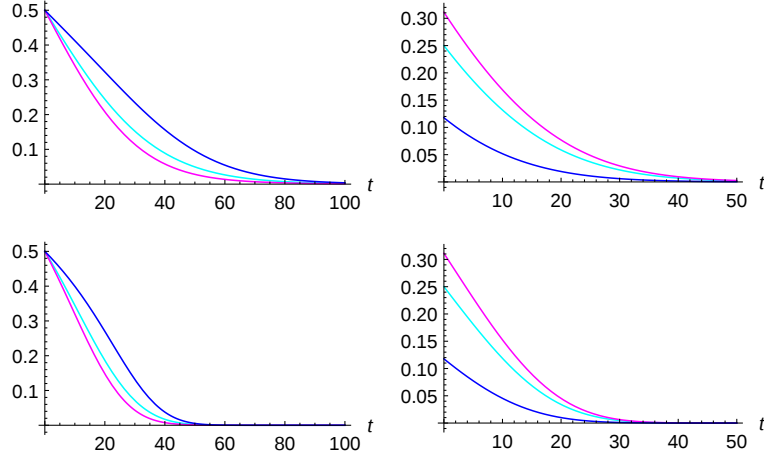


FIG. 3: Single-particle detection probability (left panels) and simultaneous detection probability (right panels) in the context of the Schrödinger equation for $g = 0$ (top panels) and $g = -0.01$ (bottom panels) for different statistics: MB (cyan curves), BE (magenta curves) and FD (blue curves). The initial parameters used are $\sigma_0 = 10$, $x_0 = 0$, $p_{0a} = 0.3$ and $p_{0b} = 0.4$.

(magenta curves) and FD (blue curves) statistics. The initial parameters used are $p_{0a} = 0.3$ and $p_{0b} = 0.55$. The probability for finding negative values of momenta of both particles is of the order of 10^{-37} for bosons and 10^{-38} for fermions meaning that the initial states (45) do not have negative-momentum contributions. This figure shows that for all kinds of particles there is just an interval for backflow even with the presence of a small opposing force. As before, this time interval becomes shorter by increasing the intensity of this force. Furthermore, although the joint detection probability for fermions is less than that for bosons and distinguishable particles, the amount of backflow is higher for fermions. With temperature and $g = 0$ (right panels), this detection probability becomes the same for the three statistics of particles at long times, being again a persistent effect with the fermions displaying a higher amount of backflow. It seems like the nature of the particles plays no role in the free propagation at long times. Note that in this limit, from Eqs. (38), (39), (51) and (52), one has that

$$\Pr_{\pm}(t) \Big|_{x_1 \& x_2 \in (-\infty, 0]} \simeq \frac{N_{\pm}^2}{2} \left\{ 1 \pm e^{-(p_{0a}-p_{0b})^2 \sigma_0^2 / \hbar^2} \right\} \approx \frac{1}{4} \quad (55)$$

where the value of $1/4$ comes from assuming $p_{0a} = 0.3$ and $p_{0b} = 0.55$. For negative g values, the complementary error function becomes zero at long times implying a zero joint detection probability in this limit for all kinds of particles.

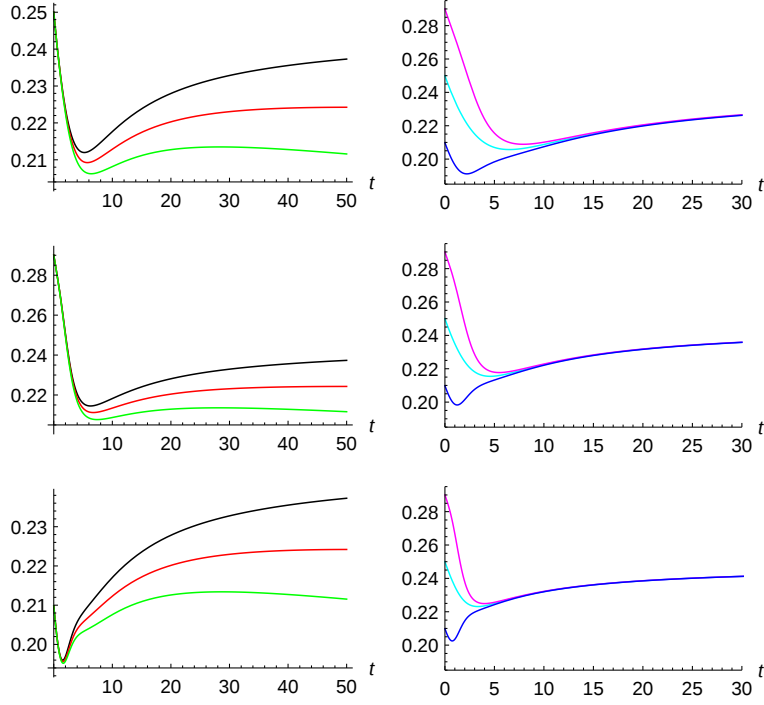


FIG. 4: The simultaneous detection probability of both particles in region $x \leq 0$, Eq. (52), versus time for $k_B T = 10$ (left panels) and for different statistics: MB (left top panel), BE (left middle panel) and FD (left bottom panel) for $g = 0$ (black curves), $g = -0.01$ (red curves) and $g = -0.02$ (green curves). The same quantity has been plotted for $g = 0$ in right panels for different values of temperatures: $k_B T = 5$ (right top panel), $k_B T = 15$ (right middle panel) and $k_B T = 40$ (right bottom panel) for MB (cyan curves), BE (magenta curves) and FD (blue curves). The initial parameters used are $\sigma_0 = 10$, $x_0 = 0$, $p_{0a} = 0.3$, $p_{0b} = 0.55$ and $\gamma = 0.1$.

Finally, Figure 5 displays the single-particle detection probability for finding a single particle in $x \leq 0$, Eq. (53), versus time with $\gamma = 0.1$ for $k_B T = 10$ (left panels) and for different statistics: MB (left top panel), BE (left middle panel) and FD (left bottom panel) with $g = 0$ (black curves), $g = -0.01$ (red curves) and $g = -0.02$ (green curves). The same probability is plotted for $g = 0$ on the right panels for different values of temperatures: $k_B T = 15$ (right top panel), $k_B T = 20$ (right middle panel) and $k_B T = 25$ (right bottom panel) for MB (cyan curves), BE (magenta curves) and FD (blue curves). The initial parameters used are $\sigma_0 = 10$, $x_0 = 0$, $p_{0a} = 0.3$, $p_{0b} = 0.4$ and $\gamma = 0.1$. As mentioned above, with these parameters, the contribution of negative momenta to the initial wave functions is negligible. Again, there is just an interval of backflow for small values of g . Both ac-

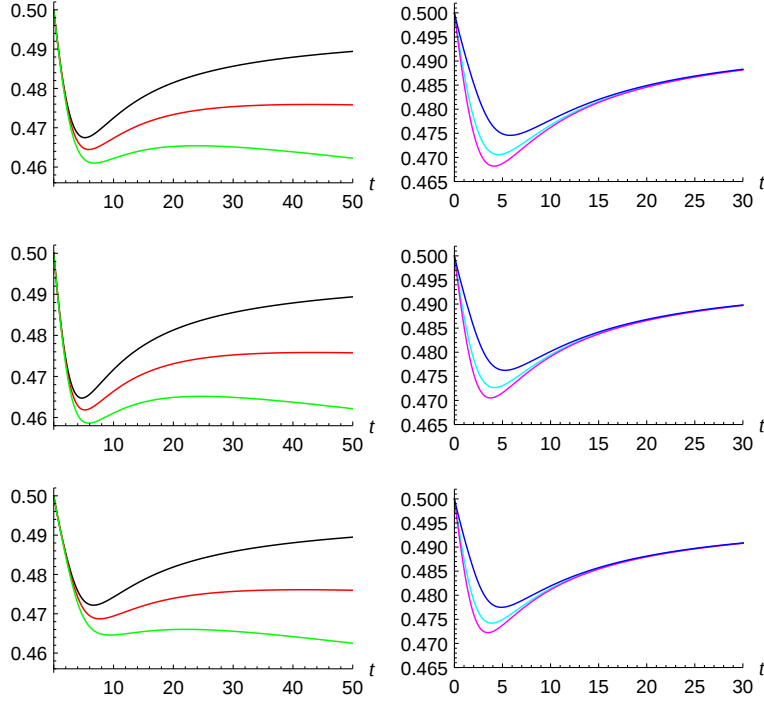


FIG. 5: Single-particle detection probability for finding a single particle in $x \leq 0$, Eq. (53), versus time for $k_B T = 10$ (left panels) and for different statistics: MB (left top panel), BE (left middle panel) and FD (left bottom panel) for $g = 0$ (black curves), $g = -0.01$ (red curves) and $g = -0.02$ (green curves). The same quantity has been plotted for $g = 0$ in right panels for different values of temperatures: $k_B T = 15$ (right top panel), $k_B T = 20$ (right middle panel) and $k_B T = 25$ (right bottom panel) for MB (cyan curves), BE (magenta curves) and FD (blue curves). Parameters have been chosen as $\sigma_0 = 10$, $x_0 = 0$, $p_{0a} = 0.3$, $p_{0b} = 0.4$ and $\gamma = 0.1$.

celeration and temperature diminish the amount of backflow. The single-particle detection probability is higher for fermions than for bosons and distinguishable particles. However, all kinds of particles behave asymptotically similar at long times, and the single-particle detection probability approaches 0.5 for $g = 0$ while becomes zero for non-zero negative g . This is apparent from Eq. (53). One has for $g = 0$ that

$$\Pr_{\pm}(t) \Big|_{x_1 \& x_2 \in (-\infty, 0]} \simeq N_{\pm}^2 \left\{ 1 \pm e^{-(p_{0a} - p_{0b})^2 \sigma_0^2 / \hbar^2} \right\} \approx \frac{1}{2} \quad (56)$$

where the value of $1/2$ comes from assuming $p_{0a} = 0.3$ and $p_{0b} = 0.4$.

This general study seems to indicate that the quantum statistics plays an important role in this effect since the amount of backflow is higher for fermions than bosons when

one considers the joint detection portability. However, when the decoherence process is gradually settled in the free propagation regime the nature of the particles is no longer relevant. Furthermore, it seems that the well-known properties of bunching for bosons and anti-bunching for fermions tend to disappear. In the free propagation regime, quantum backflow is persistent at asymptotic times reaching a constant value independent on the nature of the particles.

VI. CONCLUDING REMARKS

Backflow is a quite astonishing effect in quantum mechanics but it is curiously far less known that, for example, the tunneling effect. Although one can see non-zero amount of backflow in the limit $\hbar \rightarrow 0$, Bracken and Melloy [2] stated that this effect is a characteristic of the quantum mechanical description in terms of complex wave function; density matrix in our case, with no classical analogue. At least two reasons which could be argued are, first it has not been experimentally observed yet, and second no clear application has been still devised. However, at fundamental level, the appearance or not of backflow can be a good check to see the degree of quantumness of a given system, either closed or open.

In this work, quantum backflow has been studied for open systems in the CL formalism under the presence of an opposing force by using wave packets different to the standard Gaussian ones; in particular, we have used the stretching Gaussian and two non-Gaussian wave packets. This was motivated by our previous work [16] that backflow could occur for only a single Gaussian wave packet in the same formalism. The origin of backflow is therefore no longer due to an interference process, which requires at least two wave packets, when open quantum systems are considered. With these single wave packets, there is just a time-interval of backflow which becomes persistent at long times only for the free propagation regime while it is finite when a small opposing force is acting. Furthermore, we have found that the stretching parameter and the degree of non-Gaussianity go against of the amount of backflow.

In order to complete our study, we have extended our theoretical formalism to the case of two particle systems where the so-called joint detection and single particle detection probabilities have been evaluated when the one-particle states are assumed to be Gaussian wave packets. The amount of backflow has been shown to be higher for identical spinless

fermions than identical spinless bosons and distinguishable particles. Thus, our numerical results make clear that the quantum statistics plays an important role in this effect. However, when the decoherence process (which has been induced with the presence of damping and temperature) is gradually settled in the free propagation regime, the nature of the particles is no longer relevant. Furthermore, in the free propagation regime, quantum backflow is persistent at asymptotic times reaching a constant value independent on the nature of the particles.

Acknowledgements SVM acknowledges support from the University of Qom and SMA support from the Ministerio de Ciencia, Innovación y Universidades (Spain) under the Project FIS2017-83473-C2-1-P.

-
- [1] G. R. Allcock, Ann. Phys **53**, 253 (1969); *ibid* **53**, 286 (1969); *ibid* **53**, 311 (1969).
 - [2] A. J. Bracken and G. F. Melloy, J. Phys. A Math. Gen. **27**, 2197 (1994).
 - [3] J. G. Muga and C. R. Leavens, Phys. Rep. **338**, 353 (2000).
 - [4] M. Palmero, E. Torrontegui, J. G. Muga, and M. Modugno, Phys. Rev. A **87**, 053618 (2013).
 - [5] A. J. Bracken and G. F. Melloy, Ann. Phys. (Leipzig) **7**, 726 (1998).
 - [6] M. Penz, G. Grübl, S. Kreidl and R. Verch, J. Phys. A **39**, 423 (2006).
 - [7] M. V. Berry and S. Popescu, J. Phys. A:Math. Theor. **39**, 6965 (2006).
 - [8] M. V. Berry, J. Phys. A: Math. Theor. **43**, 415302 (2010).
 - [9] J. M. Yearsley, J. J. Halliwell, R. Hartshorn and A. Whitby, Phys. Rev. A **86**, 042116 (2012).
 - [10] J. M. Yearsley and J. J. Halliwell, J. Phys.: Conference Serie **442**, 012055 (2013).
 - [11] F. Albarelli, T. Guaita and M. G. A. Paris, Int. J. Quantum Inf., **14**, 1650032 (2016).
 - [12] M. Moshinsky, Phys. Rev. **88**, 625 (1952).
 - [13] A. Goussev, Phys. Rev. A **99**, 043626 (2019).
 - [14] H. Bostelmann, D. Cadamuro, and G. Lechner, Phys. Rev. A **96**, 012112 (2017).
 - [15] J. M. Yearsley, Phys. Rev. A **82**, 012116 (2010)
 - [16] S.V. Mousavi and S. Miret-Artés, Eur. Phys. J. Plus **135**, 324 (2020)
 - [17] P. Caldirola Nuovo Cimento **18**, 393 (1941); E. Kanai Prog. Theor. Phys. **3**, 440 (1948).
 - [18] A. O. Caldeira and A. J. Leggett, Physica A **121**, 587 (1983).

- [19] A.O. Caldeira, *An Introduction to Macroscopic Quantum Phenomena and Quantum Dissipation* (Cambridge University Press, Cambridge, 2014)
- [20] C. D. Richardson, P. Schlagheck, J. Martin, N. Vandewalle and T. Bastin, Phys. Rev. A **89**, 032118 (2014).
- [21] S.V. Mousavi and S. Miret-Artés, Eur. Phys. J. Plus **135**, 83 (2020).
- [22] A. Venugopalan, Phys. Rev. A **50**, 2742 (1994) .
- [23] A. Venugopalan, D. Kumar and R. Ghosh, Physica A **220**, 563 (1995)